TIGIT predominantly regulates the immune response via regulatory T cells

Sema Kurtulus,[1] Kaori Sakuishi,[1] Shin-Foong Ngiow,[2,3] Nicole Joller,[1] Dewar J. Tan,[1] Michele W.L. Teng,[2,3] Mark J. Smyth,[2,3] Vijay K. Kuchroo,[1] and Ana C. Anderson[1]

[1]Evergrande Center for Immunologic Diseases and Ann Romney Center for Neurologic Diseases, Brigham and Women's Hospital and Harvard Medical School, Boston, Massachusetts, USA.

[2]QIMR Berghofer Medical Research Institute, Brisbane, Queensland, Australia. [3]School of Medicine, University of Queensland, Brisbane, Queensland, Australia.

Coinhibitory receptors are critical for the maintenance of immune homeostasis. Upregulation of these receptors on effector T cells terminates T cell responses, while their expression on Tregs promotes their suppressor function. Understanding the function of coinhibitory receptors in effector T cells and Tregs is crucial, as therapies that target coinhibitory receptors are currently at the forefront of treatment strategies for cancer and other chronic diseases. T cell Ig and ITIM domain (TIGIT) is a recently identified coinhibitory receptor that is found on the surface of a variety of lymphoid cells, and its role in immune regulation is just beginning to be elucidated. We examined TIGIT-mediated immune regulation in different murine cancer models and determined that TIGIT marks the most dysfunctional subset of CD8$^+$ T cells in tumor tissue as well as tumor-tissue Tregs with a highly active and suppressive phenotype. We demonstrated that TIGIT signaling in Tregs directs their phenotype and that TIGIT primarily suppresses antitumor immunity via Tregs and not CD8$^+$ T cells. Moreover, TIGIT$^+$ Tregs upregulated expression of the coinhibitory receptor TIM-3 in tumor tissue, and TIM-3 and TIGIT synergized to suppress antitumor immune responses. Our findings provide mechanistic insight into how TIGIT regulates immune responses in chronic disease settings.

Introduction

T cell responses are controlled by multiple receptors: while costimulatory receptors ensure optimal T cell activation and proliferation to generate a protective immune response, coinhibitory or checkpoint receptors dampen effector T cell responses to prevent immunopathology and autoimmunity. In addition to their expression on effector T cells, coinhibitory receptors are also expressed on Tregs, where they serve to promote Treg suppressor function, thus further contributing to control of the immune response. How coinhibitory receptors in these different cell types achieve their effects and the relative contribution of their functions to immune regulation is still largely unknown.

Achieving a better understanding of how individual coinhibitory receptors regulate the immune response is critical, as therapeutic strategies that interfere with signaling through these receptors are currently at the forefront of treatment for cancer and other chronic diseases such as chronic viral infection. In chronic diseases, the dysregulated expression of coinhibitory receptors on effector T cells is associated with a dysfunctional effector phenotype characterized by deficits in proliferative capacity, secretion of proinflammatory cytokines, and cytotoxicity (1). Moreover, the high expression levels of coinhibitory receptors on Tregs is associated with potent Treg suppressor function. Accordingly, therapies that target the coinhibitory receptors CTLA-4 and PD-1 are proving successful in treating cancer (2). The mechanisms by which these therapies achieve their effects are still being elucidated. In this regard, a recent study showed that the response to PD-1 blockade is much higher if there are preexisting CD8$^+$ T cells within the tumor tissue (3); however, whether the recovery of productive immunity after treatment is due to direct modulation of effector T cell function or modulation of Treg function is unclear.

TIGIT is a novel coinhibitory receptor that, together with CD226 (DNAM-1), comprises a pathway that closely parallels the CD28/CTLA-4 pathway. Similar to CD28 and CTLA-4, CD226 and TIGIT share ligands (CD112 and CD155) (4–6), and engagement of CD226 enhances T cell activation (7, 8), while engagement of TIGIT inhibits T cell responses (4, 9, 10). CD226 is expressed on NK cells and CD8$^+$ T cells and is preferentially expressed on IFN-γ–producing CD4$^+$ Th1 T cells (11). TIGIT is upregulated on CD4$^+$ and CD8$^+$ T cells upon activation and is also found on NK cells, memory T cells, follicular Th cells, and on a subset of Tregs (4, 5, 9, 10, 12).

Over the past few years, TIGIT has emerged as an important coinhibitory receptor. An initial study indicated that TIGIT inhibits T cell responses indirectly by triggering CD155 in DCs, thereby preventing DC maturation and inducing production of the immunosuppressive cytokine IL-10 (4). However, recent studies show that TIGIT has a T cell–intrinsic inhibitory function in that TIGIT ligation directly inhibits T cell proliferation and cytokine production in CD4$^+$ T cells (9, 10). Similarly, TIGIT ligation also suppresses the cytolytic activity of NK cells (6). Indeed, TIGIT contains 2 immunoreceptor tyrosine-based inhibitory motifs (ITIMs) in its cytoplasmic tail (4, 10). These motifs have been shown to mediate recruitment of the phosphatase SHIP-1 (13), thus providing a mechanism by which TIGIT can act cell intrinsically to dampen activating signals. In addi-

Conflict of interest: Mark J. Smyth has a scientific research agreement with Bristol-Myers Squibb and is a paid consultant for F-star, Kymab, and Amgen.
Submitted: January 26, 2015; **Accepted:** August 17, 2015.
Reference information: *J Clin Invest.* doi:10.1172/JCI81187.

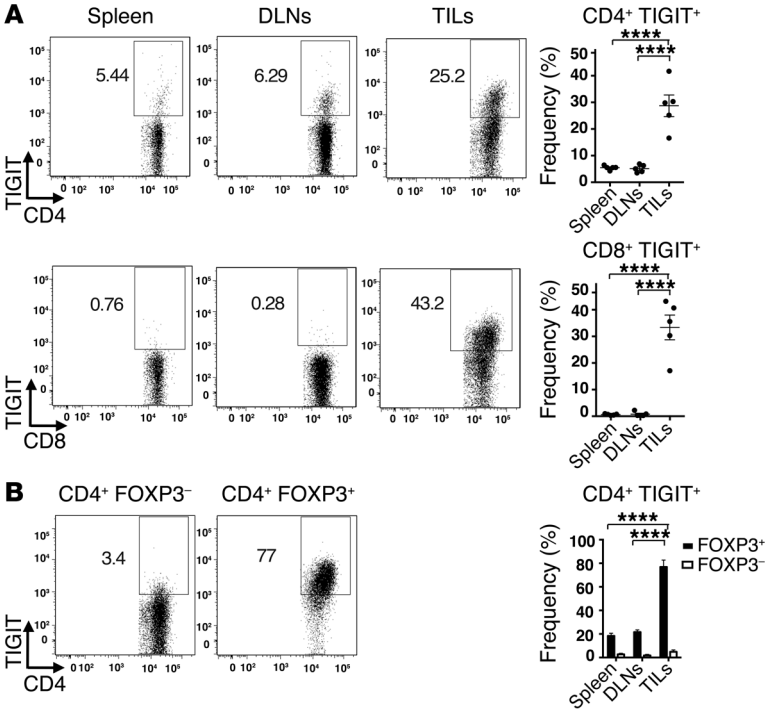

Figure 1. TIGIT is enriched on TILs. Spleen, tumor DLNs, and TILs were harvested from WT *Foxp3*-GFP–KI mice (n = 5) bearing B16F10 melanoma tumors and stained with Abs against CD4, CD8, and TIGIT. (**A**) Left panels: representative flow cytometric data showing TIGIT expression on CD4$^+$ and CD8$^+$ T cells in spleen, DLNs, and TILs. Right panel: frequency ± SEM of TIGIT$^+$ cells. ****$P < 0.0001$ by 1-way ANOVA and Tukey's multiple comparisons test. (**B**) Left panels: representative flow cytometric data showing TIGIT expression in CD4$^+$ FOXP3$^-$ (GFP$^-$) and CD4$^+$ FOXP3$^+$ (GFP$^+$) in TILs. Right panel: frequency ± SEM of TIGIT$^+$ FOXP3$^-$ and FOXP3$^+$ cells. CD4$^+$ FOXP3$^+$ percentages within total CD4$^+$ T cells were 32.46% ± 4.27%. Data are representative of 2 to 3 experiments. ****$P < 0.0001$ by 1-way ANOVA and Tukey's multiple comparisons test comparing TIGIT$^+$ FOXP3$^+$ cells across the indicated tissues.

tion to direct regulation of effector T cell responses, recent studies show that TIGIT marks a subset of Tregs that exhibit heightened expression of known Treg effector molecules and heightened suppressive capacity in vitro (12, 14). Most interestingly, TIGIT$^+$ Tregs exhibit a specialized function, that of selectively suppressing proinflammatory Th1 and Th17 responses but sparing Th2 responses (12), thus supporting a role for TIGIT in directing Treg function.

The absence of TIGIT has been shown to exacerbate experimental autoimmune encephalomyelitis, while TIGIT engagement has been shown to ameliorate collagen-induced arthritis (9, 10). Recently, blockade of TIGIT has been shown to synergize with PD-1/PD-L1 blockade to enhance antitumor CD8$^+$ T cell responses in both humans and mice (15, 16). These observations support an important inhibitory role for TIGIT in vivo; however, they do not address the role of TIGIT in effector T cells versus Tregs in regulating antitumor immunity. Here, we dissect the role of TIGIT in cancer, where coinhibitory receptor expression on effector T cells is associated with the development of T cell dysfunction, and expression on Tregs is associated with potent Treg suppressor function. We found that TIGIT is uniquely enriched on tumor-infiltrating lymphocytes (TILs), where it marks the most dysfunctional CD8$^+$ T cells and FOXP3$^+$ tumor tissue Tregs. Importantly, we show that it is not the function of TIGIT in effector CD8$^+$ T cells but rather its function in FOXP3$^+$ Tregs that plays a critical role in dampening antitumor immune responses. Our data shed light on the mechanisms by which the coinhibitory receptor TIGIT determines immune responses in chronic disease settings and highlight the therapeutic value of targeting TIGIT in cancer.

Results

TIGIT expression is upregulated on TILs. Before examining a potential role for TIGIT in regulating antitumor T cell responses, we first examined the expression of TIGIT and its ligands on several murine cancer cell lines. We found that the TIGIT ligands CD112 and CD155 were highly expressed on multiple murine cancer cell lines, while TIGIT itself was not (Supplemental Figure 1; supplemental material available online with this article; doi:10.1172/JCI81187DS1). Similarly, expression of CD155 and CD112 has also been reported in human melanoma cell lines (17). We next examined TIGIT expression on lymphocytes in mice bearing B16F10 melanoma tumors. We observed that while TIGIT was expressed at low levels on T cells in the spleen and tumor-draining lymph nodes (DLNs), it was markedly enriched on both CD4$^+$ and CD8$^+$ T cells that infiltrated melanoma tumors (Figure 1A). We further found that TIGIT was similarly enriched on the CD4$^+$ and CD8$^+$ T cells that infiltrated CT26 colon carcinoma (Supplemental Figure 2A). As TIGIT is constitutively expressed on a subset of Tregs (4, 10, 12), we further examined whether TIGIT expression was enriched on Tregs within CD4$^+$ TILs. We found that TIGIT was highly expressed on FOXP3$^+$ Tregs compared with that observed on FOXP3$^-$ CD4$^+$ TILs in both B16 melanoma (Figure 1B) and CT26 colon carcinoma (Supplemental Figure 2B). Thus, TIGIT expression was enriched on both CD8$^+$ T cells and Tregs in 2 different preclinical cancer models, and, importantly, TIGIT$^+$ lymphocytes were mostly confined to tumor tissue.

TIGIT$^+$ CD8$^+$ TILs display a dysfunctional phenotype. Coinhibitory receptors are often expressed on T cells that exhibit a dysfunctional phenotype. We therefore examined whether TIGIT$^+$ CD8$^+$ TILs display defects in effector functions. We found that TIGIT$^+$ CD8$^+$ TILs were poor producers of IL-2 and TNF-α but produced similar levels of IFN-γ compared with TIGIT$^-$ CD8$^+$ TILs (Figure 2A). Interestingly, while TIGIT$^+$ CD8$^+$ TILs exhibited deficits in proinflammatory cytokine production, we found that they had significantly increased production of the immune-suppressive cytokine IL-10 compared with TIGIT$^-$ CD8$^+$ TILs. Moreover, we found that TIGIT$^+$ CD8$^+$ TILs exhibited a reduced capacity to degranu-

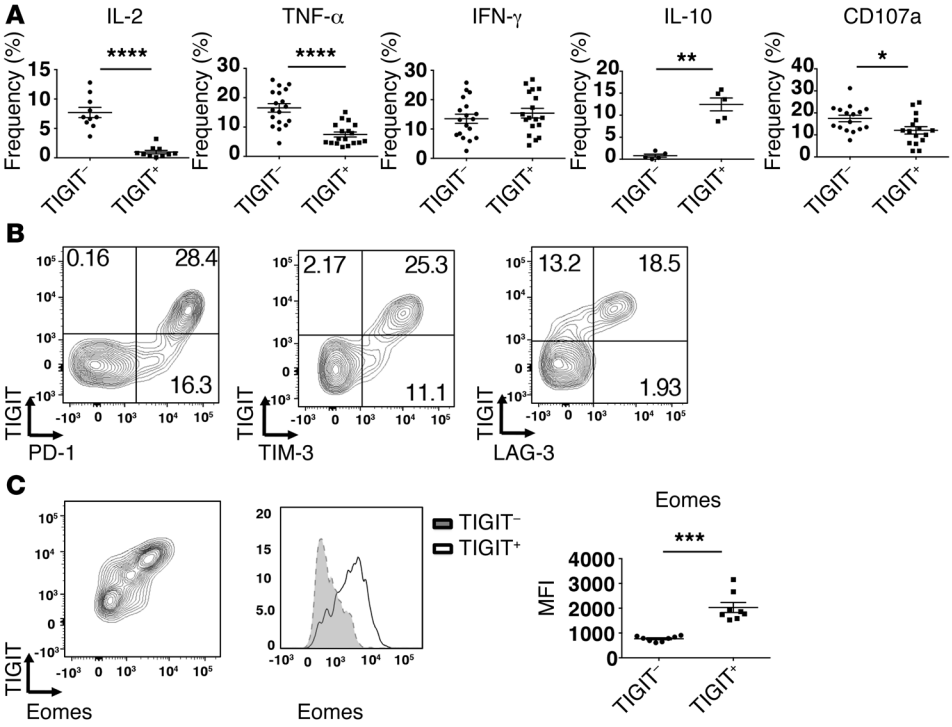

Figure 2. TIGIT marks a dysfunctional CD8⁺ T cell subset. TILs were harvested from WT mice (n = 5–20) or IL-10 Thy1.1 mice (n = 5) bearing B16F10 melanoma 12–15 days after tumor implantation when tumor sizes measured between 140 and 180 mm^2. (**A**) Frequency ± SEM of CD8⁺ TIGIT⁺ and TIGIT⁻ TILs producing IL-2, TNF-α, IFN-γ, and IL-10 (Thy1.1) or expressing surface CD107a after stimulation with anti-CD3 and anti-CD28. Data were pooled from 3 different experiments. (**B**) Representative flow cytometric data showing TIGIT coexpression with PD-1, TIM-3, and LAG-3 on CD8⁺ TILs. Data are representative of 5 individual mice. (**C**) Left panel: representative contour plot showing TIGIT coexpression with eomes in CD8⁺ TILs. Middle panel: representative histogram showing eomes expression in TIGIT⁺ and TIGIT⁻ CD8⁺ TILs. Right panel: mean fluorescence intensity (MFI) ± SEM for eomes in TIGIT⁺ and TIGIT⁻ CD8⁺ TILs (n = 8 mice). Data were pooled from 2 different experiments. ****$P < 0.0001$, ***$P < 0.001$, **$P < 0.01$, and *$P < 0.05$ by Mann-Whitney U test.

late, as determined by surface expression of CD107a, when compared with TIGIT⁻ CD8⁺ TILs (Figure 2A). Together, these data show that TIGIT⁺ CD8⁺ TILs are dysfunctional and further suggest that, in addition to being poor mediators of tumor clearance, they may contribute to immune suppression locally in the tumor microenvironment by virtue of their enhanced production of IL-10.

The accumulation of multiple coinhibitory receptors on the surface of T cells is associated with increased dysfunction (18). We therefore examined the expression of TIGIT in conjunction with other coinhibitory receptors (PD-1, LAG-3, and TIM-3) that have been associated with a dysfunctional phenotype in TILs (19–22). We found that TIGIT was coexpressed with PD-1, TIM-3, and LAG-3 on CD8⁺ TILs (Figure 2B). Interestingly, we observed that TIGIT was expressed on CD8⁺ TILs that exhibited the highest levels of PD-1 and TIM-3. In chronic lymphocytic choriomeningitis virus (LCMV) infection, where T cell dysfunction has been well studied, it has been shown that high expression of PD-1 coincides with high expression of the transcription factor Eomes and that PD-1^{hi} Eomes^{hi} CD8⁺ T cells constitute a terminally exhausted subset that exhibits severe dysfunction (23). Recently, PD-1^{hi} Eomes^{hi} CD8⁺ T cells have also been described in melanoma tumors and found to exhibit decreased function (24). As TIGIT coincides with high PD-1 expression on CD8⁺ TILs (Figure 2B), we examined whether these cells also exhibit high expression of eomes. Indeed, we found that TIGIT⁺ CD8⁺ TILs had significantly higher expression of eomes compared with that observed on TIGIT⁻ CD8⁺ TILs (Figure 2C). Collectively, our data show that TIGIT⁺ CD8⁺ T cells constitute a highly dysfunctional subset within CD8⁺ TILs.

TIGIT⁺ Tregs exhibit a highly activated and suppressive phenotype in tumor tissue. Our data show that TIGIT expression within CD4⁺ TILs was almost exclusively on FOXP3⁺ Tregs (Figure 1B). Recently, TIGIT expression was shown to identify a cell population within natural Tregs that exhibits a highly activated and suppressive Treg phenotype (12). Accordingly, we examined whether TIGIT⁺ Tregs in tumor tissue exhibited a more activated phenotype than did their TIGIT⁻ Treg counterparts. For this, we determined the expression profile of more than 200 immunologically relevant genes in TIGIT⁺ versus TIGIT⁻ Tregs isolated from melanoma tumors using NanoString nCounter technology. We identified several genes that were differentially regulated in TIGIT⁺ relative to TIGIT⁻ Tregs isolated from tumor tissue (Figure 3A and complete list in Supplemental Table 1). Many of these genes are consistent with those previously reported as differentially regulated in TIGIT⁺ Tregs relative to TIGIT⁻ Tregs in naive mice (12). Similarly upregulated genes included genes that encode coinhibitory receptors (*Pdcd1*, which encodes PD-1, *Lag3*, *Ctla4*, and *Havcr2*, which encodes TIM-3), chemokines and chemokine receptors (*Ccr2*, *Ccr5*, *Ccr8*, *Cxcr3*, *Cxcr6*, and *Ccl5*), transcription factors (*Rora*, *Prdm1*, *Id2*, *Tbx21*, and *Foxp3*), and the effector molecule *Il10*. Similarly downregulated genes included *Bcl2*, *Tcf7*, and *Ifngr2*.

Among the most highly upregulated genes in TIGIT⁺ Tregs from TILs was *Il10* (Figure 3A). As IL-10 is an important Treg effector molecule in vivo, we confirmed that the TIGIT⁺ Tregs from TILs are indeed major producers of IL-10 by examining the TIGIT⁺ and TIGIT⁻ Tregs isolated from TILs of tumor-bearing IL-10/FOXP3 reporter mice (Figure 3B). We further found that other Treg effector molecules (*Prf1*, which encodes perforin, and TGF-β1) are also more highly expressed in TIGIT⁺ than in TIGIT⁻ Tregs in TILs. Collectively, our data indicate that TIGIT⁺ Tregs in TILs exhibit a highly activated suppressor phenotype relative to their TIGIT⁻ Treg counterparts. Indeed, we found that the TIGIT⁺ Tregs in TILs were more suppressive compared with the TIGIT⁻ Tregs in TILs (Figure 3C).

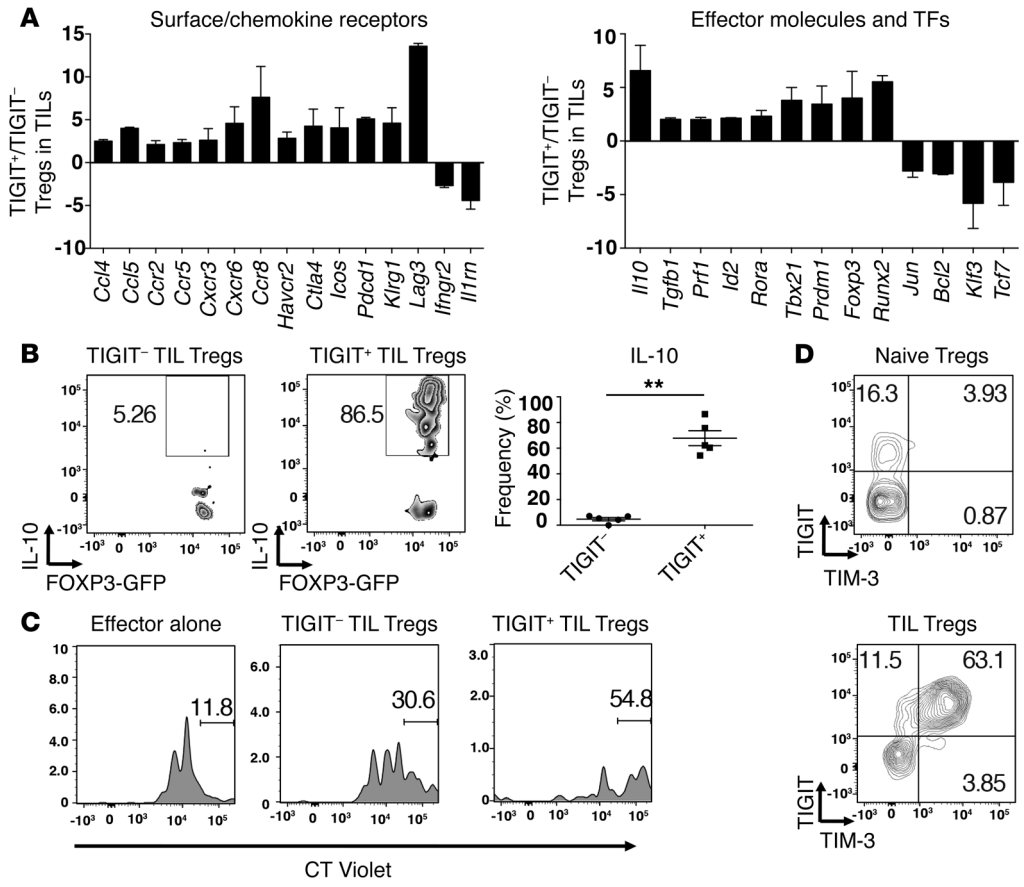

Figure 3. TIGIT⁺ Tregs in the tumor tissue exhibit a more suppressive and activated phenotype. TIGIT⁺ and TIGIT⁻ Tregs were isolated from B16F10 tumors implanted into *Foxp3*-GFP–KI mice (**A**, **C**, and **D**) or IL-10-Thy1.1 *Foxp3*-GFP–KI mice (**B**). (**A**) Gene expression was analyzed using a custom NanoString CodeSet. Bar graphs show the fold expression ± SEM of selected differentially expressed surface receptors (left), effector molecules, and transcription factors (TFs) (right) in TIGIT⁺ and TIGIT⁻ Tregs. Data are pooled from 2 different experiments. Selected genes with a fold change of greater than 2 are depicted. (**B**) Left panels: representative flow cytometric data showing IL-10-Thy1.1 staining in TIGIT⁻ and TIGIT⁺ Treg TILs. Right panel: frequency ± SEM of IL-10⁺ cells within TIGIT⁻ and TIGIT⁺ Treg TILs ($n = 5$). Data are representative of 2 independent experiments. $^{**}P < 0.01$ by Mann-Whitney *U* test. (**C**) Tregs isolated from tumor tissue were cocultured with splenic CT Violet–labeled CD4⁺ T cells (1:8). CT Violet dilution was analyzed by flow cytometry 4 days later. Gates indicate the undivided CD4⁺ subsets. Data are representative of 2 experiments. (**D**) Representative contour plots of TIM-3 expression on TIGIT⁺ TIL Tregs or TIGIT⁺ naive Tregs. Data are representative of 5 individual mice.

Among the genes upregulated in TIGIT⁺ Tregs in TILs, *Havcr2* was of particular interest, as we had previously found that TIM-3 is uniquely enriched on Tregs that accumulate in tumor tissue and express high levels of both IL-10 and perforin (25). Examination of TIM-3 and TIGIT expression in Tregs from naive and tumor-bearing mice showed that while TIM-3 was expressed on a fraction of TIGIT⁺ Tregs in naive mice, all of the TIGIT⁺ Tregs in tumor tissue expressed TIM-3, and at a much higher level than that observed in naive Tregs (Figure 3D). The potent upregulation of TIM-3 in tumor tissue, together with the highly active and suppressive Treg phenotype of TIGIT⁺ Tregs in tumor tissue, raises the possibility that the TIM-3 and TIGIT signaling pathways may cooperate to direct Treg function in tumor tissue.

Enhanced antitumor immunity in the absence of TIGIT. Our data show that TIGIT expression marks severely dysfunctional CD8⁺ TILs and tumor tissue Tregs that exhibit a highly activated and suppressive phenotype (Figures 2 and 3); however, they do not address whether TIGIT has a role in regulating antitumor immunity. To address this, we monitored tumor growth in germline TIGIT–deficient (*Tigit*$^{-/-}$) mice. We found that TIGIT deficiency significantly delayed the growth of both B16F10 melanoma and MC38 colon carcinoma relative to WT controls (Figure 4A), indicating that TIGIT plays an inhibitory role in different tumor models. As TIGIT can be expressed by NK cells as well as by CD8⁺ T cells (4–6), we determined whether the enhanced antitumor immunity observed in the absence of TIGIT was dependent on CD8⁺ T cell or NK cell responses. Using depleting Abs, we found that CD8⁺ T cells, but not NK cells, were required for the improved control of tumor growth observed in the absence of TIGIT (Figure 4B). To address whether better control of tumor growth in the absence of TIGIT indeed correlated with increased function in CD8⁺ TILs, we examined antigen-specific responses in CD8⁺ TILs from mice bearing B16F10 melanoma tumors. We found that both the frequency of granzyme B⁺ cells as well as the expression level of granzyme B was increased in CD8⁺ TILs from *Tigit*$^{-/-}$ mice after stimulation (Figure 4C). We further examined the effect of TIGIT deficiency on antigen-specific cytokine responses in either B16F10 melanoma or MC38 colon carcinoma

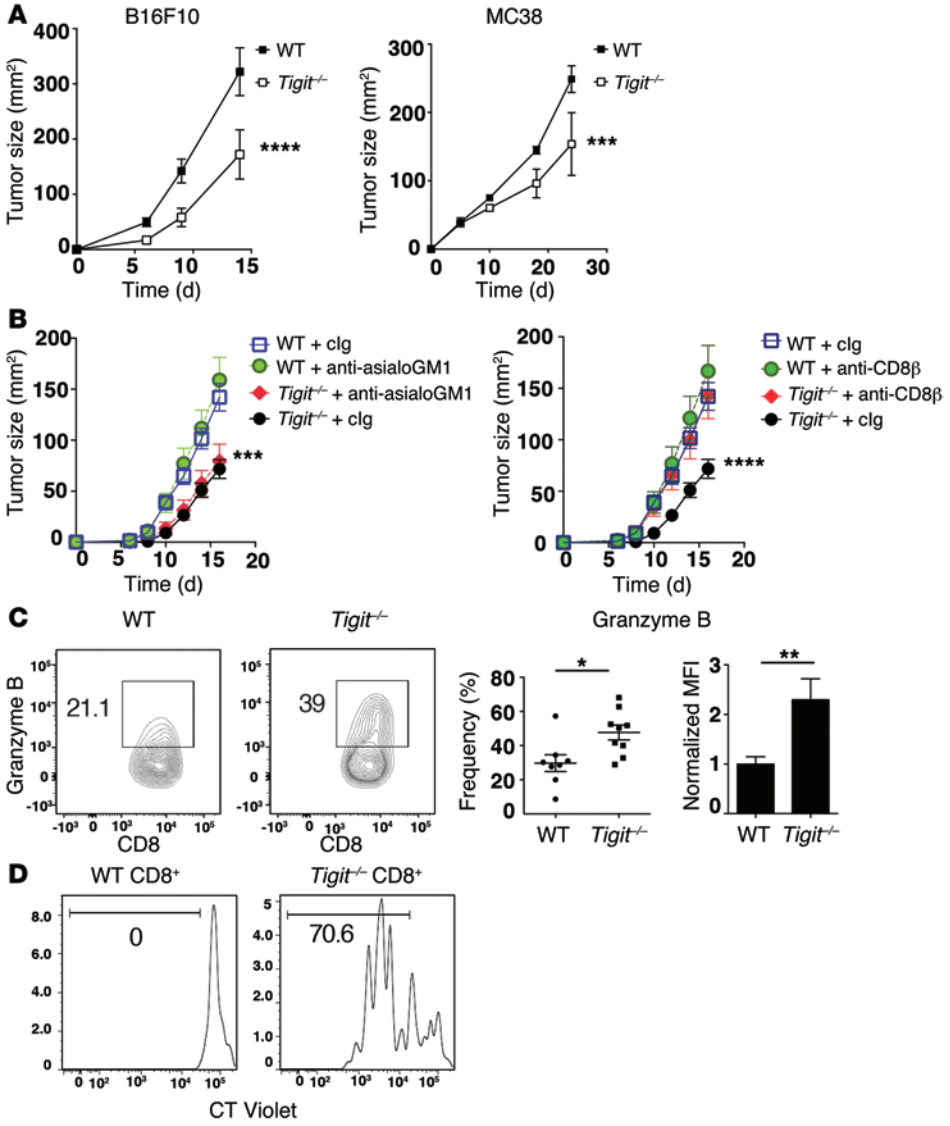

Figure 4. TIGIT restrains antitumor immune responses. (**A**) Growth of B16F10 melanoma or MC38 colon carcinoma in WT or *Tigit*$^{-/-}$ mice (n = 5–6). Data are representative of 3 independent experiments. ***P < 0.001 and ****P < 0.0001 by repeated-measures ANOVA with a Sidak test. (**B**) WT or *Tigit*$^{-/-}$ mice (n = 5) were treated i.p. with anti-asialoGM1 or anti-CD8β Abs or with their isotype controls (clg) on days –1, 0, 7, and 14 after B16F10 tumor implantation. Tumor growth after anti-asialoGM1 (left) or anti-CD8β (right) treatment is shown. Data are representative of 2 independent experiments. Comparisons are between WT plus clg versus *Tigit*$^{-/-}$, irrespective of clg or anti-asialoGM1 treatment (left), and between clg versus anti-CD8β in *Tigit*$^{-/-}$ mice (right). ***P < 0.001 and ****P < 0.0001 by repeated-measures ANOVA with a Sidak test. (**C** and **D**) Total TILs were isolated from B16F10 tumor–bearing WT or Tigit$^{-/-}$ mice (n = 4–5). (**C**) TILs were stimulated with 10 μg/ml gp100 peptide. Contour plots and bar graphs show the percentage ± SEM of granzyme B$^+$ cells and the normalized MFI of granzyme B expression within CD8$^+$ TILs. MFI was normalized to the mean of WT CD8$^+$ TILs in each independent experiment. Data were pooled from 2 to 3 experiments. *P < 0.05 and **P < 0.01 by Mann-Whitney U test. (**D**) CT Violet–labeled TILs were stimulated with anti-CD3 for 4 days and then analyzed by flow cytometry. Representative histogram of CT Violet dilution in CD8$^+$ TILs. Data are representative of 3 individual measurements.

engineered to express low levels of OVA (MC38-OVA^{dim}) (26) and observed a trend toward higher frequencies of IL-2–, TNF-α–, and IFN-γ–producing cells within TILs from TIGIT-deficient mice (Supplemental Figure 3, A and B). Last, we found that while WT CD8$^+$ TILs exhibited little to no proliferation after stimulation with anti-CD3, *Tigit*$^{-/-}$ CD8$^+$ TILs exhibited a heightened proliferative response (Figure 4D). Collectively, these data support the idea that TIGIT limits antitumor T cell responses.

TIGIT$^+$ Tregs regulate antitumor immunity. While our data support the idea that TIGIT has a role in the regulation of antitumor CD8$^+$ T cell responses (Figure 4), they do not elucidate whether TIGIT suppresses antitumor CD8$^+$ T cells directly or indirectly via Tregs. To address this question, we established an adoptive transfer system using WT and TIGIT-deficient (*Tigit*$^{-/-}$) T cells, wherein we could segregate the loss of TIGIT expression to either CD8$^+$ T cells or CD4$^+$ FOXP3$^+$ Tregs. To address the role of TIGIT in CD8$^+$ T cells, we adoptively transferred WT CD4$^+$ T cells (FOXP3$^+$ and FOXP3$^-$) along with either WT or *Tigit*$^{-/-}$ CD8$^+$ T cells into *Rag*-deficient (*Rag*$^{-/-}$) mice that were subsequently implanted with B16F10 melanoma. We found that the mice that received *Tigit*$^{-/-}$ CD8$^+$ T cells showed similar tumor growth compared with mice that received WT CD8$^+$ T cells (Figure 5A). We next addressed the role of TIGIT in Tregs by transferring WT or *Tigit*$^{-/-}$ (CD4$^+$ FOXP3$^+$) Tregs along with WT CD4$^+$ effector (FOXP3$^-$) and WT CD8$^+$ effector T cells. In contrast to our observations in mice harboring TIGIT deficiency only in CD8$^+$ T cells, we found that mice that received *Tigit*$^{-/-}$ Tregs exhibited significantly delayed tumor growth compared with mice that received WT Tregs (Figure 5B). Given this difference in tumor growth, we examined whether lack of TIGIT in Tregs interfered with the development of a dysfunctional phenotype in CD8$^+$ T cells. As TIGIT expression on CD8$^+$ TILs correlated with a highly dysfunctional phenotype (Figure 2), we determined TIGIT expression on CD8$^+$ TILs in mice that received WT or *Tigit*$^{-/-}$ Tregs. We found a significant decrease in the frequency of TIGIT$^+$ CD8$^+$ TILs in mice harboring TIGIT deficiency in Tregs, indicating that the absence of TIGIT in Tregs restrains the development of a severe dysfunctional phenotype in CD8$^+$ TILs (Figure 5C). Indeed, we found that lack of TIGIT on Tregs resulted in significantly enhanced IL-2, TNF-α, and IFN-γ production by CD8$^+$ TILs (Figure 5D).

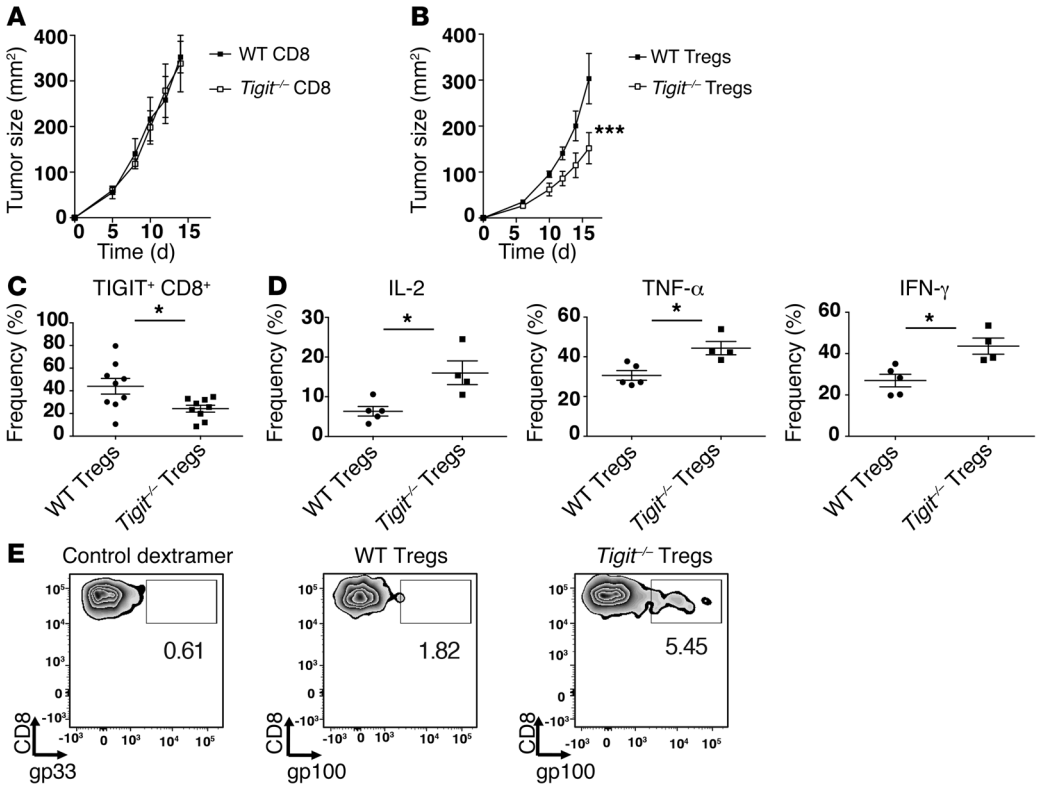

Figure 5. TIGIT expression on Tregs has a dominant role compared with CD8⁺ T cells in regulating antitumor responses. (**A**) CD8⁺ T cells from WT or *Tigit*$^{-/-}$ mice were mixed with WT CD4⁺ (FOXP3⁺ and FOXP3⁻) T cells and injected i.v. into *Rag*$^{-/-}$ mice (n = 5). Two days later, mice were implanted with B16F10 tumor cells. Graph shows tumor growth over time. Data are representative of 3 different experiments. (**B**) Tregs from WT or *Tigit*$^{-/-}$ *Foxp3*-GFP–KI mice were mixed with WT CD8⁺ and CD4⁺ FOXP3⁻ cells and transferred into *Rag*$^{-/-}$ mice (n = 5). Graph shows tumor growth over time. Data are representative of 5 different experiments. ***$P < 0.001$ by repeated-measures ANOVA with a Sidak test. (**C**–**E**) Seventeen days after implantation, TILs and DLNs were isolated from mice that received WT or *Tigit*$^{-/-}$ Tregs. (**C**) Frequency ± SEM of TIGIT⁺ CD8⁺ TILs from each group (n = 9–10). Data were pooled from 2 independent experiments. (**D**) TILs were stimulated with anti-CD3 and anti-CD28 and analyzed for cytokine production. Graphs show IL-2⁺, TNF-α⁺, and IFN-γ⁺ percentages ± SEM within CD8⁺ TILs in each group (n = 4–5). *$P < 0.05$ by Mann-Whitney U test (**C** and **D**). (**E**) Representative plots show gp33 (control dextramer) or gp100 dextramer staining in CD8⁺ T cells from pooled DLNs of *Rag*$^{-/-}$ mice. (**D** and **E**) Data are representative of 2 independent experiments.

Last, we found that the frequency of gp100-specific CD8⁺ T cells was also increased in mice harboring TIGIT deficiency only in Tregs, suggesting that the maintenance and/or survival of antigen-specific CD8⁺ T cells is enhanced in the absence of TIGIT on Tregs (Figure 5E). Together, these data indicate that TIGIT dampens antitumor immunity predominantly by regulating Treg function, which in turn promotes the development of a severe dysfunctional phenotype in CD8⁺ T cells.

TIGIT signaling in Tregs. Our data support a key role for TIGIT in suppressing antitumor immunity via its role in Tregs. This raises the important question of how TIGIT signaling alters the Treg phenotype. While our examination of the gene expression profile of TIGIT⁺ Tregs in TILs showed increased expression of Treg effector molecules and upregulation of some distinct genes relative to TIGIT⁻ Tregs (Figure 3), it did not address whether engagement of TIGIT is responsible for driving the differential expression of any of these genes. The likelihood that TIGIT is actively engaged in the tumor environment is high, given our observation of the elevated expression levels of TIGIT ligands on tumor cells (Supplemental Figure 1). To address the possibility that TIGIT engagement might modulate the Treg phenotype in tumor tissue, we identified the genes that are downstream of TIGIT signaling in Tregs. For this, we used an agonistic anti-TIGIT Ab that was previously shown to bind to TIGIT and inhibit T cell proliferation (9). We stimulated Tregs in vitro in the presence of the agonistic anti-TIGIT Ab and examined gene expression at 2 different time points (48 and 96 hours) using NanoString nCounter technology as described above. We found several genes that were modulated in Tregs as a consequence of TIGIT signaling (Figure 6). We also found that the transcription factors *Eomes*, *Irf8*, *Prdm1*, *Tbx21*, and *Runx2* were induced by TIGIT signaling in Tregs. TIGIT ligation also upregulated expression of the chemokine *Ccl4* and the chemokine receptors *Cxcr3* and *Ccr8*. The upregulation of *Cxcr3* and *Tbx21* indicates that TIGIT signaling may direct suppressor function toward IFN-γ–producing T cells, as T-bet⁺ CXCR3⁺ Tregs have been shown to control Th1 type inflammation in vivo (27). The upregulation of *CCR8* and *CCL4* indicates that TIGIT signaling may promote Treg migration and retention in tumor tissue (28, 29). Interestingly, TIGIT signaling decreased expression of *TCF7*, which has recently been shown to antagonize the FOXP3-driven transcriptional program in Tregs (30). Thus, TIGIT signaling in Tregs may favor Treg stability. In line with this observation, TIGIT expression has recently been shown to correlate strongly with a stable Treg phenotype in humans (14). Importantly, several of the

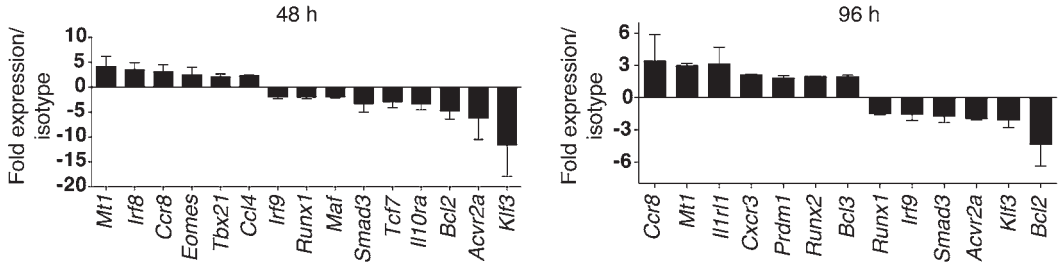

Figure 6. TIGIT signaling in Tregs. CD4$^+$ FOXP3$^+$ Tregs from WT *Foxp3*-GFP–KI mice were sorted and stimulated with plate-bound isotype or agonistic anti-TIGIT Ab, together with anti-CD3 and anti-CD28, for 48 or 96 hours. Gene expression was then analyzed using a NanoString CodeSet. Bar graphs show the fold expression ± SEM of genes in Ab-treated versus isotype-treated cells at 48 and 96 hours. Data were pooled from 2 different experiments.

genes we identified as modulated upon TIGIT signaling in Tregs (*Tbx21*, *Ccr8*, *Ccl4*, *Cxcr3*, *Prdm1*, *Runx2*, *Klf3*, *Bcl2*, and *Tcf7*) were among the genes we observed as differentially regulated in TIGIT$^+$ relative to TIGIT$^-$ Tregs from TILs (Figure 3A and Supplemental Table 1). Collectively, these data support the notion that TIGIT actively signals in Tregs to modulate the Treg phenotype and that TIGIT is actively engaged in vivo in the tumor microenvironment.

TIGIT synergizes with TIM-3. Our data showing TIM-3 upregulation on TIGIT$^+$ Tregs in tumor tissue (Figure 3), together with our data indicating the dominant function of TIGIT in Tregs in suppressing antitumor immunity (Figure 5), raised the possibility that the TIGIT and TIM-3 pathways might act synergistically to drive suppression in the tumor environment. We therefore examined the effect of TIM-3 blockade in the absence of TIGIT and found that treatment of *Tigit*$^{-/-}$ mice with anti–TIM-3 Abs significantly decreased tumor growth compared with *Tigit*$^{-/-}$ deficiency alone (Figure 7A). As observed in WT versus *Tigit*$^{-/-}$ mice (Figure 4B), the synergistic effect of anti–TIM-3 in *Tigit*$^{-/-}$ mice required CD8$^+$ T cells but not NK cells (Supplemental Figure 4). We further tested anti–TIM-3 in *Tigit*$^{-/-}$ and WT mice in 2 different models of experimental tumor metastasis and found that TIM-3 blockade further reduced the number of foci in the lungs of *Tigit*$^{-/-}$ mice (Figure 7B). Last, TIM-3 blockade increased survival over that observed with TIGIT deficiency alone in a B16F10 melanoma lung metastasis model (Figure 7C). Collectively, these data support the idea that TIM-3 and TIGIT cooperate to suppress antitumor responses.

Discussion

Our data add a dimension to our current understanding of how TIGIT modulates antitumor immunity by showing that the function of TIGIT in Tregs is dominant over its function in CD8$^+$ T cells. This observation runs counter to the emphasis on the role of coinhibitory receptors in suppressing antitumor immunity via the direct promotion of a dysfunctional phenotype in CD8$^+$ T cells. Instead, our data suggest that TIGIT signaling induces a molecular program in Tregs that in turn drives the development of a dysfunctional phenotype in CD8$^+$ T cells. This observation is in line with our previous study showing that the dysfunctional phenotype of CD8$^+$ TILs is diminished after Treg depletion (25) and with a recent study showing that Tregs modify the tumor microenvironment to promote CD8$^+$ T cell dysfunction (31). Similarly, Tregs have recently been shown to play an important role in the maintenance of T cell dysfunction in chronic LCMV infection (32). Thus, a key function of Tregs in chronic disease settings may be to drive the dysfunctional phenotype in effector CD8$^+$ T cells in order to prevent immunopathology. Our data indicate that TIGIT signaling may be critical for the role of Tregs in driving CD8$^+$ T cell dysfunction.

One possible mechanism by which TIGIT$^+$ Tregs can drive a dysfunctional phenotype in effector T cells is via their high production of IL-10. Our data show that IL-10 is among the genes most highly upregulated in TIGIT$^+$ Tregs that infiltrate tumor tissue. Indeed, IL-10 has been linked to viral persistence and the development of T cell dysfunction in chronic LCMV infection (33, 34). Further elucidation of the transcriptome of TIGIT$^+$ Tregs from tumor tissue will likely identify other potential mechanisms by which TIGIT$^+$ Tregs can drive T cell dysfunction.

The dominant function of TIGIT in Tregs in immune regulation is reminiscent of the role of CTLA-4 on Tregs. CTLA-4 has been shown to be critical for the maintenance of Treg suppressor function (35). However, unlike CTLA-4, which is expressed on all Tregs, TIGIT is only expressed on a subset of normal circulating Tregs (12) and, as we show here, is highly enriched on the Tregs that infiltrate tumor tissue. The enriched expression of TIGIT in tumor tissue positions TIGIT as a more precise molecular target than is CTLA-4. Thus, therapies that target TIGIT would be expected to result in fewer unwanted systemic effects than would those that target CTLA-4 (2) and function via Treg depletion (36–38).

Importantly, our data do not exclude a direct role for TIGIT in promoting a dysfunctional phenotype in CD8$^+$ T cells. Indeed, it is possible that the combined loss of TIGIT in Tregs and CD8$^+$ T cells would have an even stronger effect on tumor immunity than would loss of TIGIT in Tregs alone. The fact that TIGIT deficiency in CD8$^+$ T cells alone does not result in improved antitumor immunity likely reflects compensation by other coinhibitory receptors that are functionally redundant with TIGIT. Functional redundancy across coinhibitory receptor pathways would not be surprising in the tumor microenvironment, where there is strong pressure to keep CD8$^+$ T cell responses suppressed and CD8$^+$ T cells express multiple coinhibitory receptors. Indeed, such functional redundancy forms the basis for why coblockade of coinhibitory receptors has been shown to be more effective in both preclinical cancer models and the clinic (39–41).

A recent study suggests that TIGIT regulates T cell function by inhibiting CD226 dimerization and downstream signaling (15). Our study does not exclude this possibility. Rather, our data support the notion that TIGIT signaling drives a cell-intrinsic gene program in Tregs that suppresses antitumor effector T cell responses. In addition to Treg-intrinsic TIGIT signaling, it is also possible that

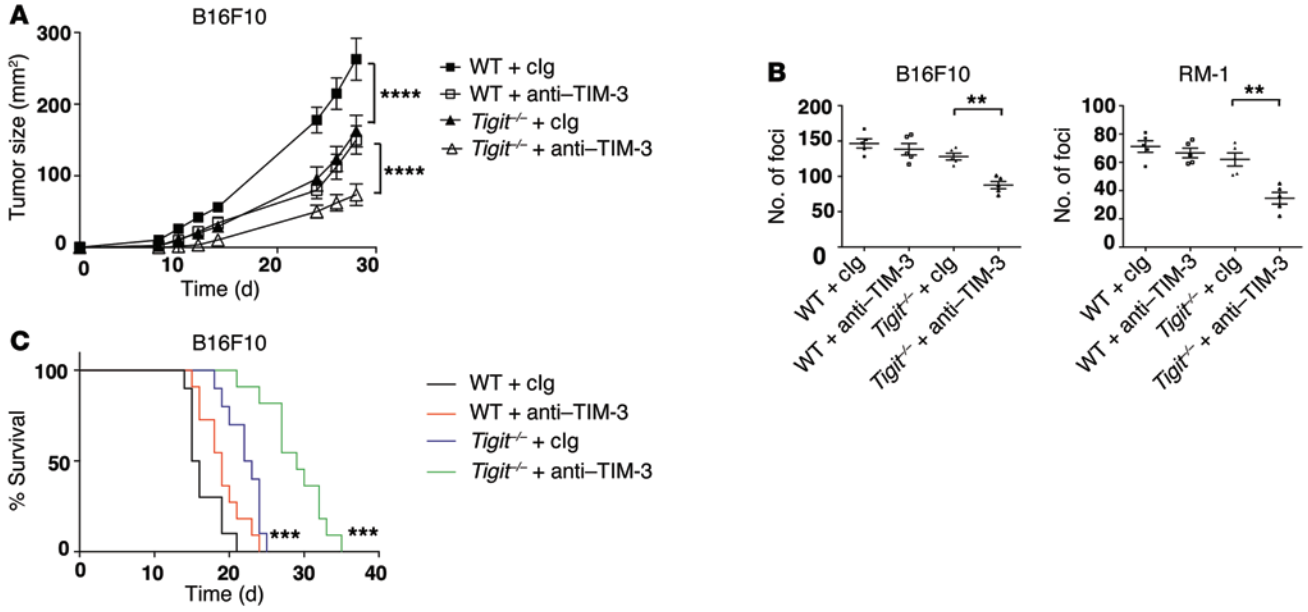

Figure 7. TIM-3 and TIGIT synergize to suppress antitumor immunity. (**A**) WT and *Tigit*$^{-/-}$ mice (n = 5) were implanted s.c. with B16F10 melanoma cells and treated with 250 μg isotype or anti–TIM-3 (RMT3-23) Ab on days 3, 6, 9, and 12. Statistical comparisons are between WT plus Ig and *Tigit*$^{-/-}$ plus Ig and between *Tigit*$^{-/-}$ plus Ig and *Tigit*$^{-/-}$ plus anti–TIM-3. ****P < 0.0001 by repeated-measures ANOVA with a Sidak test. Data are representative of 2 experiments. (**B** and **C**) B16F10 melanoma cells or RM-1 cells were administered i.v. to WT mice (n = 5 per group) that were treated i.p. with 250 μg isotype (clg) and/or anti–TIM-3 (RMT3-23) Ab on days 0 and 3. (**B**) Graphs show the number of foci ± SEM in the lungs after B16F10 (left) or RM-1 (right) cell injections on day 14. Statistical comparisons are between *Tigit*$^{-/-}$ plus clg and *Tigit*$^{-/-}$ plus anti–TIM-3. **P < 0.01 by Mann-Whitney U test. Data are representative of 2 experiments. (**C**) Survival of mice (n = 10 per group) after i.v. administration of B16F10 melanoma cells. Statistical comparisons are between WT plus clg and *Tigit*$^{-/-}$ plus clg and between *Tigit*$^{-/-}$ plus clg and *Tigit*$^{-/-}$ plus anti–TIM-3. ***P < 0.001 by log-rank test. Data were pooled from 2 independent experiments.

the interaction of TIGIT with CD155 on antigen-presenting cells (APCs) in the tumor environment has an important role in regulating antitumor immunity. Indeed, Tregs are known to modify the DC phenotype (42), and TIGIT engagement of CD155 in DCs has been shown to inhibit IL-12 and enhance IL-10 production (4). Whether TIGIT$^+$ Tregs interact with tumor-associated DCs and induce them to become tolerogenic will be the subject of future studies.

The distinct role TIGIT plays in different subsets of TILs is an important consideration for combinatorial immunotherapeutic approaches involving TIGIT blockade. A recent study showed that anti-TIGIT controls tumor growth much more efficiently when combined with anti–PD-1 (15). In light of our data, the remarkable efficacy of TIGIT/PD-1 coblockade could reflect the combined effect of direct modulation of dysfunctional CD8$^+$ T cells, together with modulation of highly suppressive intratumoral Tregs. Our data further suggest that cotargeting TIGIT and TIM-3 could be another potent combined immunotherapeutic approach. Further investigation will be required to determine whether the TIGIT, PD-1, and TIM-3 pathways synergize at the cellular level in CD8$^+$ T cells, Tregs, or both. Our observations broaden the current perspective of how therapies that target the coinhibitory receptor TIGIT modulate antitumor immunity.

Methods

Mice. Six- to eight-week-old female BALB/c, C57BL/6, and *Rag2*$^{-/-}$ mice were purchased from The Jackson Laboratory. *Foxp3*-GFP–knockin (KI) reporter mice (43), IL-10–CD90.1 reporter mice (44), and *Tigit*$^{-/-}$ mice (10) were previously described. *Tigit*$^{-/-}$ mice were provided by ZymoGenetics (Bristol-Myers Squibb).

Cell lines. CT26, B16F10, LLC, and MC38 cell lines were purchased from ATCC. MC38-OVA^{dim} was derived from MC38 as previously described (26).

Isolation of TILs. TILs were isolated by dissociating tumor tissue in the presence of collagenase D (2.5 mg/ml) for 20 minutes prior to centrifugation on a discontinuous Percoll gradient (GE Healthcare). Isolated cells were then used in various assays of T cell function. Cells were cultured in DMEM supplemented with 10% (vol/vol) FCS, 50 μM 2-mercaptoethanol, 1 mM sodium pyruvate, nonessential amino acids, L-glutamine, and 100 U/ml penicillin and 100 μg/ml streptomycin.

Flow cytometry. Single-cell suspensions were stained with Abs against surface molecules. CD4 (clone RM4-5), CD8 (clone 53-6.7), and PD-1 (clone RMP1-30) Abs were purchased from BioLegend. LAG-3 (clone C9B7W) and TIGIT (clone GIGD7) Abs were purchased from eBioscience. TIM-3 (clone 5D12) Ab was generated in-house. Staining with gp100 dextramers (Immudex) was done according to the manufacturer's protocol. Fixable viability dye eF506 (eBioscience) was used to exclude dead cells. For CD107a staining, TILs were stimulated with anti-CD3 (0.5 μg/ml) and anti-CD28 (0.25 μg/ml) (BioLegend) for 4 hours in the presence of Golgi stop (BD Biosciences) and CD107a Ab (clone 1D4B) (BioLegend). For intracytoplasmic cytokine staining, cells were stimulated with anti-CD3 and anti-CD28 as described above. For granzyme B staining, TILs from B16F10 tumors were stimulated with 10 μg/ml hgp100, harvested, and stained with Abs against surface proteins prior to fixation and permeabilization. Permeabilized cells were then stained with Abs against IL-2 (clone JES6-5H4), TNF-α (clone MP6-XT22), IFN-γ (clone XMG-1.2) (eBioscience), or granzyme B (clone 2C5/F5; BD Pharmingen). For IL-10 detection, TILs were isolated from IL-10 Thy1.1 reporter mice, and after 4 hours of stimulation,

cells were stained with Abs against Thy1.1 (clone OX-7; BioLegend). For eomes staining, cells were stained with Abs against surface proteins and fixed and permeabilized with an eBioscience FOXP3 staining kit and then stained with anti-Eomes (clone Dan11mag) Ab (eBioscience). To assess cell proliferation, TILs were labeled with CellTrace (CT) Violet (Life Technologies) and stimulated with 0.5 μg/ml anti-CD3 for 4 days and then stained and analyzed by flow cytometry. All data were collected on a BD LSR II flow cytometer (BD Biosciences) and analyzed with FlowJo software.

Suppression assay. Tregs were isolated from tumor tissue of *Foxp3*-GFP–KI reporter mice by cell sorting on a BD FACSAria. Effector $CD4^+$ T cells were isolated from spleens of WT unimmunized mice with anti-CD4 beads (Miltenyi Biotec) and labeled with CT Violet dye. Tregs were cocultured with effector $CD4^+$ T cells at a 1:8 ratio. Irradiated splenic APCs were added to cocultures at a 5:1 ratio (APC/effector $CD4^+$) with anti-CD3 (1 μg/ml). Cells were analyzed by flow cytometry 4 days later.

Tumor experiments. CT26 and MC38 (1×10^6) or B16F10 (5×10^5) cells were implanted s.c. into the right flank. Tumor size was measured in 2 dimensions by caliper and is expressed as the product of 2 perpendicular diameters. In some experiments, mice were treated i.p. with 100 μg anti-asialoGM1 or anti-CD8β (clone 53.5.8; BioLegend) Abs or with their isotype controls (cIg) on days –1, 0, 7, and 14 after B16F10 implantation. In some experiments, mice were treated with 250 μg isotype (rat IgG2a) or anti–TIM-3 (clone RMT3-23; Bio X Cell) Abs on the days indicated in the legend for Figure 7. In some experiments, 1×10^5 B16F10 melanoma cells or RM-1 prostate cancer cells were administered i.v. to WT mice. Metastatic burden was quantified by counting the number of foci on the surface of the lungs 14 days after injection. In some experimental metastatic model experiments, mice were monitored to determine survival.

Adoptive transfers. For adoptive transfer experiments, $CD4^+$ ($FOXP3^+$ and $FOXP3^-$) and $CD8^+$ T cells from either WT or *Tigit*$^{-/-}$ *Foxp3*-GFP–KI reporter mice were isolated by cell sorting using a BD FACSAria. A total of 1.5×10^6 cells at a ratio of 1:0.5:0.01 (CD4/CD8/Treg) was mixed in PBS and injected i.v. into *Rag*$^{-/-}$ mice. Two days later, mice were implanted with B16F10 melanoma cells and followed for tumor growth.

Analysis of gene expression by NanoString. $CD4^+$ $FOXP3^+$ $TIGIT^+$ and $TIGIT^-$ cells were isolated by cell sorting from the TILs of *Foxp3*-GFP–KI mice bearing B16F10 melanoma tumors on day 10 after tumor implantation. For the examination of TIGIT signaling, $CD4^+$ $FOXP3^+$ cells from naive *Foxp3*-GFP–KI mice were isolated by cell sorting and stimulated with plate-bound anti-CD3 (1 μg/ml) and anti-CD28 (2 μg/ml), together with either agonist anti-TIGIT (4D4, generated in-house, ref. 9) (50 μg/ml) or isotype control. After 48 and 96 hours, cells were lysed in RLT lysis buffer (QIAGEN) and lysates hybridized with a custom-made CodeSet. Barcodes were counted (1,150 fields of view per sample) on an nCounter Digital Analyzer following the manufacturer's protocol (NanoString Technologies Inc.). Data were processed first by normalization with respect to the geometric mean of the positive control spike counts (provided by the manufacturer) and then with 4 reference genes (*Actb*, *Gapdh*, *Hprt*, and *Tubb5*). A background correction was done by subtracting the mean plus 2 SDs of the 8 negative control counts (provided by the manufacturer) and eliminating data that were less than 1.

Statistics. Statistical differences were determined using GraphPad Prism software. Statistical significance was calculated by Mann-Whitney *U* test for pair-wise comparisons. For multiple comparisons, a 1-way ANOVA test was performed, and pair-wise significance was determined by Tukey's multiple comparisons test. For assessment of the differences between tumor growth curves, significance was calculated by a repeated-measures ANOVA test, followed by a Sidak correction test. Statistical differences between survival curves were calculated by log-rank test. Values of $P < 0.0001$, $P < 0.001$, $P < 0.01$, and $P < 0.05$ were considered statistically significant.

Study approval. All experiments involving laboratory animals were performed under protocols approved by the Harvard Medical Area Standing Committee on Animals (Boston, Massachusetts, USA) and the QIMR Berghofer Animal Ethics Committee (Brisbane, Queensland, Australia).

Acknowledgments

We thank ZymoGenetics for mice, Deneen Kozoriz for cell sorting, and Junrong Xia, Michelle Yong, and Kimberley Stannard for their technical assistance. This work was supported by grants from the American Cancer Society (RSG-11-057-01-LIB, to A.C. Anderson); the Melanoma Research Foundation (to A.C. Anderson); a Career Development Award from the Brigham and Women's Hospital (to A.C. Anderson); and the NIH (P01AI073748, to V.K. Kuchroo and A.C. Anderson and R01NS045937 and P01AI039671, to V.K. Kuchroo). M.J. Smyth and S.F. Ngiow were supported by a National Health and Medical Research Council (NH&MRC) Senior Principal Research Fellowship (1078671) and Development Grant (1093566) and a QIMR Berghofer Medical Research Institute Rio Tinto Ride to Conquer Cancer Grant. M.W.L. Teng was supported by a NH&MRC CDF1 Fellowship and Project Grant.

Address correspondence to: Ana C. Anderson, 77 Avenue Louis Pasteur, HIM 784, Boston, Massachusetts 02115, USA. Phone: 617.525.5850; E-mail: aanderson@rics.bwh.harvard.edu.

Nicole Joller's present address is: Institute of Experimental Immunology, University of Zürich, Zürich, Switzerland.

1. Wherry EJ. T cell exhaustion. *Nat Immunol*. 2011;12(6):492–499.
2. Page DB, Postow MA, Callahan MK, Allison JP, Wolchok JD. Immune modulation in cancer with antibodies. *Annu Rev Med*. 2014;65:185–202.
3. Tumeh PC, et al. PD-1 blockade induces responses by inhibiting adaptive immune resistance. *Nature*. 2014;515(7528):568–571.
4. Yu X, et al. The surface protein TIGIT suppresses T cell activation by promoting the generation of mature immunoregulatory dendritic cells. *Nat Immunol*. 2009;10(1):48–57.
5. Boles KS, et al. A novel molecular interaction for the adhesion of follicular CD4 T cells to follicular DC. *Eur J Immunol*. 2009;39(3):695–703.
6. Stanietsky N, et al. The interaction of TIGIT with PVR and PVRL2 inhibits human NK cell cytotoxicity. *Proc Natl Acad Sci U S A*. 2009;106(42):17858–17863.
7. Bottino C, et al. Identification of PVR (CD155) and Nectin-2 (CD112) as cell surface ligands for the human DNAM-1 (CD226) activating molecule. *J Exp Med*. 2003;198(4):557–567.
8. Tahara-Hanaoka S, et al. Functional characterization of DNAM-1 (CD226) interaction with its ligands PVR (CD155) and nectin-2 (PRR-2/CD112). *Int Immunol*. 2004;16(4):533–538.
9. Joller N, et al. Cutting edge: TIGIT has T cell-intrinsic inhibitory functions. *J Immunol*. 2011;186(3):1338–1342.

10. Levin SD, et al. Vstm3 is a member of the CD28 family and an important modulator of T-cell function. *Eur J Immunol*. 2011;41(4):902–915.
11. Dardalhon V, et al. CD226 is specifically expressed on the surface of Th1 cells and regulates their expansion and effector functions. *J Immunol*. 2005;175(3):1558–1565.
12. Joller N, et al. Treg cells expressing the coinhibitory molecule TIGIT selectively inhibit proinflammatory Th1 and Th17 cell responses. *Immunity*. 2014;40(4):569–581.
13. Li M, et al. T-cell immunoglobulin and ITIM domain (TIGIT) receptor/poliovirus receptor (PVR) ligand engagement suppresses interferon-gamma production of natural killer cells via beta-arrestin 2-mediated negative signaling. *J Biol Chem*. 2014;289(25):17647–17657.
14. Fuhrman CA, et al. Divergent phenotypes of human regulatory T cells expressing the receptors TIGIT and CD226. *J Immunol*. 2015;195(1):145–155.
15. Johnston RJ, et al. The immunoreceptor TIGIT regulates antitumor and antiviral CD8(+) T cell effector function. *Cancer Cell*. 2014;26(6):923–937.
16. Chauvin JM, et al. TIGIT and PD-1 impair tumor antigen-specific $CD8^+$ T cells in melanoma patients. *J Clin Invest*. 2015;125(5):2046–2058.
17. Casado JG, et al. Expression of adhesion molecules and ligands for activating and costimulatory receptors involved in cell-mediated cytotoxicity in a large panel of human melanoma cell lines. *Cancer Immunol Immunother*. 2009;58(9):1517–1526.
18. Blackburn SD, et al. Coregulation of $CD8^+$ T cell exhaustion by multiple inhibitory receptors during chronic viral infection. *Nat Immunol*. 2009;10(1):29–37.
19. Blank C, Mackensen A. Contribution of the PD-L1/PD-1 pathway to T-cell exhaustion: an update on implications for chronic infections and tumor evasion. *Cancer Immunol Immunother*. 2007;56(5):739–745.
20. Grosso JF, et al. LAG-3 regulates $CD8^+$ T cell accumulation and effector function in murine self- and tumor-tolerance systems. *J Clin Invest*. 2007;117(11):3383–3392.
21. Ahmadzadeh M, et al. Tumor antigen-specific CD8 T cells infiltrating the tumor express high levels of PD-1 and are functionally impaired. *Blood*. 2009;114(8):1537–1544.
22. Sakuishi K, Apetoh L, Sullivan JM, Blazar BR, Kuchroo VK, Anderson AC. Targeting TIM-3 and PD-1 pathways to reverse T cell exhaustion and restore anti-tumor immunity. *J Exp Med*. 2010;207(10):2187–2194.
23. Paley MA, et al. Progenitor and terminal subsets of $CD8^+$ T cells cooperate to contain chronic viral infection. *Science*. 2012;338(6111):1220–1225.
24. Twyman-Saint Victor C, et al. Radiation and dual checkpoint blockade activate non-redundant immune mechanisms in cancer. *Nature*. 2015;520(7547):373–377.
25. Sakuishi K, et al. TIM3FOXP3 regulatory T cells are tissue-specific promoters of T-cell dysfunction in cancer. *Oncoimmunology*. 2013;2(4):e23849.
26. Gilfillan S, et al. DNAM-1 promotes activation of cytotoxic lymphocytes by nonprofessional antigen-presenting cells and tumors. *J Exp Med*. 2008;205(13):2965–2973.
27. Koch MA, Tucker-Heard G, Perdue NR, Killebrew JR, Urdahl KB, Campbell DJ. The transcription factor T-bet controls regulatory T cell homeostasis and function during type 1 inflammation. *Nat Immunol*. 2009;10(6):595–602.
28. Tan MC, et al. Disruption of CCR5-dependent homing of regulatory T cells inhibits tumor growth in a murine model of pancreatic cancer. *J Immunol*. 2009;182(3):1746–1755.
29. Iellem A, et al. Unique chemotactic response profile and specific expression of chemokine receptors CCR4 and CCR8 by CD4(+)CD25(+) regulatory T cells. *J Exp Med*. 2001;194(6):847–853.
30. van Loosdregt J, et al. Canonical Wnt signaling negatively modulates regulatory T cell function. *Immunity*. 2013;39(2):298–310.
31. Bauer CA, Kim EY, Marangoni F, Carrizosa E, Claudio NM, Mempel TR. Dynamic Treg interactions with intratumoral APCs promote local CTL dysfunction. *J Clin Invest*. 2014;124(6):2425–2440.
32. Penaloza-MacMaster P, et al. Interplay between regulatory T cells and PD-1 in modulating T cell exhaustion and viral control during chronic LCMV infection. *J Exp Med*. 2014;211(9):1905–1918.
33. Brooks DG, Trifilo MJ, Edelmann KH, Teyton L, McGavern DB, Oldstone MB. Interleukin-10 determines viral clearance or persistence in vivo. *Nat Med*. 2006;12(11):1301–1309.
34. Ejrnaes M, et al. Resolution of a chronic viral infection after interleukin-10 receptor blockade. *J Exp Med*. 2006;203(11):2461–2472.
35. Wing K, et al. CTLA-4 control over $Foxp3^+$ regulatory T cell function. *Science*. 2008;322(5899):271–275.
36. Selby MJ, et al. Anti-CTLA-4 antibodies of IgG2a isotype enhance antitumor activity through reduction of intratumoral regulatory T cells. *Cancer Immunol Res*. 2013;1(1):32–42.
37. Simpson TR, et al. Fc-dependent depletion of tumor-infiltrating regulatory T cells co-defines the efficacy of anti-CTLA-4 therapy against melanoma. *J Exp Med*. 2013;210(9):1695–1710.
38. Bulliard Y, et al. Activating Fcγ receptors contribute to the antitumor activities of immunoregulatory receptor-targeting antibodies. *J Exp Med*. 2013;210(9):1685–1693.
39. Pardoll DM. The blockade of immune checkpoints in cancer immunotherapy. *Nat Rev Cancer*. 2012;12(4):252–264.
40. Larkin J, et al. Combined nivolumab and ipilimumab or monotherapy in untreated melanoma. *N Engl J Med*. 2015;373(1):23–34.
41. Postow MA, et al. Nivolumab and ipilimumab versus ipilimumab in untreated melanoma. *N Engl J Med*. 2015;372(21):2006–2017.
42. Tang Q, Bluestone JA. The $Foxp3^+$ regulatory T cell: a jack of all trades, master of regulation. *Nat Immunol*. 2008;9(3):239–244.
43. Bettelli E, et al. Reciprocal developmental pathways for the generation of pathogenic effector TH17 and regulatory T cells. *Nature*. 2006;441(7090):235–238.
44. Maynard CL, et al. Regulatory T cells expressing interleukin 10 develop from $Foxp3^+$ and $Foxp3^-$ precursor cells in the absence of interleukin 10. *Nat Immunol*. 2007;8(9):931–941.